

Bidirectional multiple port dc/dc transformer based on a series resonant converter

Zoran Pavlović; Jesús A. Oliver; Pedro Alou; Óscar Garcia; José A. Cobos

I. INTRODUCTION

The research on high performance bidirectional dc/dc converters is gaining on importance, since they are key components in designing more efficient power distribution systems. In this context, multiple port converters have been attracting increased investigation effort, [1]-[3]. They are widely employed in the hybrid power distribution systems to control power flow between different power sources, storage elements and loads. Multiple port structures are also desirable from the viewpoints of cost, area and control. The power flow is typically controlled using phase shift control scheme, alone or combined with PWM control.

In order to provide power to the electronic loads that demand different supply voltages, multiple output converters can be used. Several approaches have been proposed to deliver independently and tightly regulated output voltages, [4]-[6]. Pulsewidth and complementary pulsewidth PFM modulation are used in [4] to control the output voltages. In [5] the main output voltage is controlled by the switching frequency modulation while in [6] the outputs are regulated by the phase shifting between the independent leading legs and the shared lagging leg. Besides the complex control, the solutions presented in [4] and [6] use one transformer per output and inductances to filter the output voltages, what limits converter power density.

In typical power distribution architectures the power is delivered to the load through multiple voltage buses, [7]. The

connection of each of those buses to the common input voltage is done using single-input single-output dc/dc converters. The performances of those single-input single-output dc/dc converters are key issues to determine the performances of the whole power distribution architecture. Integration of different voltage buses into a single power node leads to a reduction of the required multiple converter stages used in the conventional architectures.

This paper is aimed at integrating different converter stages, typically found in power delivery architectures, into a novel bidirectional multiple port power node to overcome the aforementioned drawbacks. The new power node topology is based on a resonant converter topology and reduces to only one the number of magnetic components. Soft switching commutations make possible high switching frequencies to be adopted and high power densities to be achieved. Possible problems regarding stray inductances are eliminated since they are absorbed into the circuit elements. The converter features very good inherent load and cross regulation due to the small output impedances. However, the input voltage regulation capability is lost since the converter is operated at its resonant frequency with 50% duty cycle. Unlike the conventional architectures where each single-input single-output dc/dc converters has its own control, the power node control is relocated and centralized to the previous stage to regulate the input voltage of the power node.

II. THE PROPOSED MULTIPLE PORT DC/DC TRANSFORMER

The proposed bidirectional multiple port dc/dc transformer is based on the series resonant converter topology, [8]-[10]. The extension of the SRC converter to the multiple output topology is achieved by adding transformer windings and the corresponding inverter/rectifier cells. An example of a three port dc/dc transformer is shown in Figure 1. It consists of a half bridge inverter on the primary side and two full bridge rectifiers on the secondary side of the high frequency transformer, that provides isolation and is framed with dashed line in Figure 1. For each port, the designer can select either a full bridge or a half bridge type inverter/rectifier to permit bidirectional power flow and optimize the converter operation. One of the key benefits of this multiple port converter is that the transformer is the only magnetic component in the design and its leakage inductances form part of the resonant tank

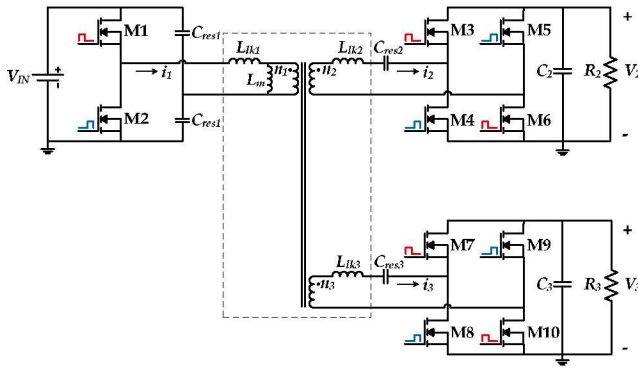


Figure 1. Three port SRC based bidirectional dc/dc transformer.

networks on both the input and the output ports. No additional inductor is required for output voltage filtering. Another advantage is that the converter is operated at fixed switching frequency with complementary and constant duty cycle (approximately 50%) switch driving signals (red and blue gate signals (v_{GS}) in Figure 2).

The switches on the opposite diagonals in the inverter cells are driven simultaneously, as it is indicated in Figure 1 with red and blue gate signals. A resonant tank at each port is comprised of the corresponding leakage inductance and a series capacitor; if the selected inverter/rectifier is the half bridge, the resonant capacitance is just provided by the half bridge capacitors themselves, i.e., the series capacitance seen by resonant inductor is the equivalent parallel connection of the half bridge capacitors. When the full bridge inverter/rectifier is used, the series capacitor is placed between the transformer and the full bridge cell. The resonant frequencies of all three resonant tank networks are tuned to the switching frequency. Reordering the well-known relation given in (1) between the tank resonant frequency, f_{sw} , and its inductance, L , and capacitance, C , the expression for the selection of the resonant capacitors C_{res1} , C_{res2} and C_{res3} is given in (2), where $i \in [1,2,3]$ and $j=0$ for full bridge and $j=1$ for half bridge inverter:

$$f_{sw} = \frac{1}{2\pi\sqrt{LC}} \quad (1)$$

$$C_{res,i} = \frac{1}{(2\pi f_{sw})^2 2^j L_{lk,i}} \quad (2)$$

A. Operating principle

Basic voltage and current waveforms of the three port dc/dc transformer when the magnetizing current is taken into account are shown in Figure 2. Due to the magnetizing current effect, the resonant tank currents have some non-zero values at the ends of each half cycle. Four operating stages can be distinguished, according to the conduction state of the switches and the magnetizing current direction.

Stage 1 [$t_0 - t_1$]: At time t_0 the switches M1, M3, M6, M7 and M10 are turned on and positive voltages $V_{IN}/2$, V_2 and V_3 are applied to the transformer primary and secondary resonant tanks. These voltages are ideally proportional to the

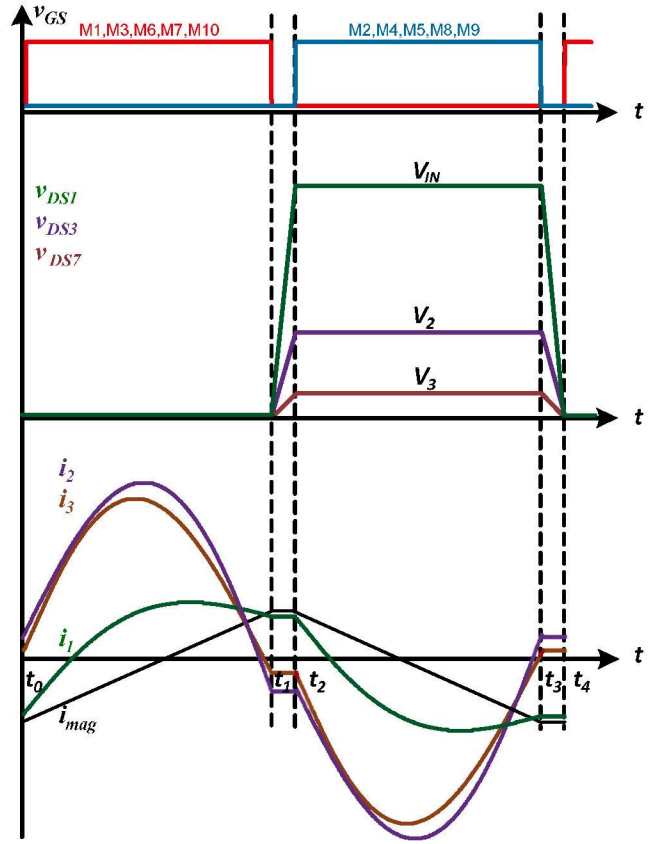


Figure 2. Voltage and current waveforms of the three port dc/dc transformer from Figure 1.

transformer turns ratio $n_0:n_1:n_2$. The slight difference between them is due to the voltage drops on the transformer and switch resistances on the current path. The higher these resistances are, the higher are the voltage drops and the differences of the output voltages, V_2 and V_3 , from their nominal values. The switches M3, M6, M7 and M10 are turned off with nearly ZCS at time t_1 when the positive sinusoidal currents i_1 and i_2 cross zero, while the switch M1 is turned off with the peak magnetizing current.

Stage 2 [$t_1 - t_2$]: During this stage the voltage across the series resonant capacitors can be considered constant since these capacitances are much higher than the parasitic capacitances. It can also be assumed that the magnetizing current is approximately constant during the dead time interval. At t_1 the positive peak magnetizing current is distributed among the primary and both secondary side tanks and discharges the capacitances $2C_{oss1}$, a parallel connection of the switches' M1 and M2 parasitic drain-source capacitances, C_{oss2} , C_{oss3} and C_p , which represents the equivalent parasitic transformer winding capacitance seen from the primary side. At time t_2 parasitic drain-source capacitances of the switches M1, M3, M6, M7 and M10 are charged to their respective voltages and the switches M2, M4, M5, M8 and M9 are discharged to be turned on with ZVS. Also, due to the redistribution of the magnetizing current between the primary and secondary sides, the switches M4, M5, M8 and M9 are turned on with small negative portion of the magnetizing current (Figure 2).

Stage 3 [$t_2 - t_3$]: In the time interval $t_2 - t_3$ a similar circuit operation as in the time interval $t_0 - t_1$ can be observed. Since all the switches are turned on with ZVS and turned off with nearly ZCS, a significant reduction in switching losses is achieved. This permits selection of high switching frequency to reduce the size of the transformer and obtain high power density.

Stage 4 [$t_3 - t_4$]: In this stage the negative peak magnetizing current charges parasitic drain-source capacitances, C_{oss} , of the switches M2, M4, M5, M8 and M9, discharges C_{oss} of M1, M3, M6, M7 and M10 and also charges parasitic self-capacitance of the transformer windings, C_p . The time interval $t_3 - t_4$ completes one switching cycle.

Unlike the single output dc/dc transformer based on SRC where only one resonant capacitor is needed to resonate with the transformer primary and secondary side leakage inductances, in case of three port dc/dc transformer three resonant capacitors are needed. Let's assume that only two resonant capacitors are selected according to (2) and the third one is omitted. If the current waveforms on the transformer sides with added resonant capacitors were sinusoidal with ZCS, there would be a voltage drop across the inductor on the side with no added capacitor and its current would be a cosine function. On the other hand, the current through the single inductor has to be sinusoidal due to the transformer current relation. Therefore, a different current distribution in the transformer windings would be established, leading to a loss of ZCS condition at turn off in all the switches and, as a consequence, switching losses would be higher. Therefore, the impact of the transformer leakage inductances at each winding has to be canceled at the switching frequency.

B. Self and cross load regulation

Another advantage of the proposed multiple port converter is a good load regulation and cross-regulation among the outputs due to its inherent low output impedances. Load variation at one output port has very small effect on its own output voltage and on the others. In order to calculate its output resistances, an equivalent circuit of the three port dc/dc transformer seen from the primary side when the power transfer occurs is shown in Figure 3. The square voltage sources, that represent the output voltage of the half bridge inverter and input voltages of the full bridge rectifiers seen from the primary side, are in phase and their values are given in Figure 3. Since all the three resonant tanks are tuned to the switching frequency, the resonant tank currents i_1 , i_2 and i_3 will contain only fundamental frequency components and the components due to the magnetizing current. It can be assumed that the currents in phase with the square voltage sources are given as in (3):

$$i_{k,ph} = I_{m,k} \sin \omega t \quad (3)$$

where $k \in [2,3]$, $\omega = 2\pi f_{sw}$ and the amplitudes $I_{m,k}$ depend on the output currents $I_{OUT,k}$, which are the average values of the rectified resonant tank currents:

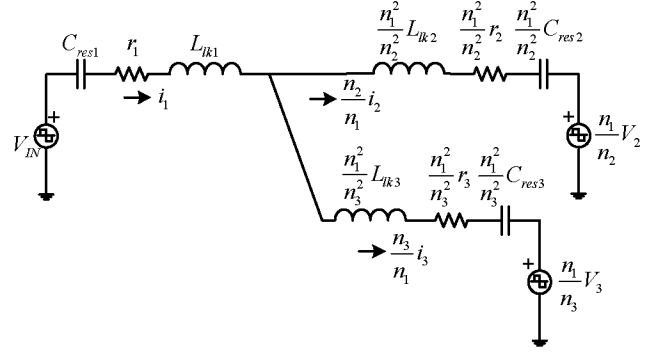


Figure 3. Equivalent circuit of the three port dc/dc transformer seen from the primary side.

$$I_{m,k} = \frac{\pi}{2} I_{OUT,k} \quad (4)$$

It can also be assumed that the voltage drop on the primary side resonant tank including the primary side switch on resistance, layout and transformer equivalent primary series resistance, r_1 , is negligible comparing to the input voltage. Therefore, it can be considered that the inverter square voltage waveform is applied across the magnetizing inductance giving its current a triangular form with the peak magnetizing current, I_{mag} , given in (5):

$$I_{mag} = \frac{V_{IN}}{8f_{sw}L_m} \quad (5)$$

The fundamental harmonic of the magnetizing current is given by (6):

$$i_m^{(1)} = -\frac{8}{\pi^2} I_{mag} \cos \omega t \quad (6)$$

By converting the sinusoidal voltage drops on the current path parasitic resistances r_1 , r_2 and r_3 into square voltages, the expressions needed to calculate the output voltages are given by (7) and (8):

$$\frac{V_{IN}}{2} - \frac{\pi}{4} r_1 \left(\frac{n_2}{n_1} I_{m,2} + \frac{n_3}{n_1} I_{m,3} \right) - \frac{\pi}{4} \frac{n_1^2}{n_2^2} r_2 \frac{n_2}{n_1} I_{m,2} - \frac{n_1}{n_2} V_2 = 0 \quad (7)$$

$$\frac{V_{IN}}{2} - \frac{\pi}{4} r_1 \left(\frac{n_2}{n_1} I_{m,2} + \frac{n_3}{n_1} I_{m,3} \right) - \frac{\pi}{4} \frac{n_1^2}{n_3^2} r_3 \frac{n_3}{n_1} I_{m,3} - \frac{n_1}{n_3} V_3 = 0 \quad (8)$$

where r_1 , r_2 and r_3 are comprised of the switch on resistances, layout and the transformer equivalent series resistance in the primary and the secondary sides circuits. After the rearrangement of the expressions (7) and (8) the output voltages are expressed by the self and mutual output resistances as in (9) and (10):

$$V_2 = \frac{n_2}{n_1} \frac{V_{IN}}{2} - \frac{\pi^2}{8} \left(\frac{n_2^2}{n_1^2} r_1 + r_2 \right) I_{OUT,2} - \frac{\pi^2}{8} \frac{n_2 n_3}{n_1^2} r_1 I_{OUT,3} \quad (9)$$

$$V_3 = \frac{n_3}{n_1} \frac{V_{IN}}{2} - \frac{\pi^2}{8} \frac{n_3 n_2}{n_1^2} r_1 I_{OUT,2} - \frac{\pi^2}{8} \left(\frac{n_3^2}{n_1^2} r_1 + r_3 \right) I_{OUT,3} \quad (10)$$

The inherent load regulation is given by those resistances that depend on the MOSFETs on-resistances, layout and transformer series resistances and can have very small values. Therefore, the output voltage deviations from their nominal values will not be significant. Besides, as the output currents decrease, the resonant tank currents also decrease making possible low losses and high efficiency operation at light load conditions to be obtained.

C. Magnetizing current effect

The square voltage sources from Figure 3 have no components that are in phase with the fundamental harmonic of the magnetizing current, $i_m^{(1)}$ and, in order to calculate the magnetizing current distribution in the resonant tanks, can be eliminated from the circuit, as well as the series connections of the resonant capacitors and leakage inductances. Besides, since the voltage across the magnetizing inductance does not change significantly, the magnetizing inductance can be considered as a current source. By using the superposition theorem, the equivalent circuit from Figure 3 can now be reduced to the one shown in Figure 4.

The currents $i_{1,m}$, $i_{2,m}$ and $i_{3,m}$ depend only on the current path resistances in the primary and secondary circuits and the transformer turn ratio and can be easily calculated. The total input and output currents are:

$$i_1 = \frac{n_2 i_{2,ph} + n_3 i_{3,ph}}{n_1} + \frac{1}{1 + r_1 \left(\frac{n_2^2}{n_1^2 r_2} + \frac{n_3^2}{n_1^2 r_3} \right)} i_m^{(1)} \quad (11)$$

$$i_2 = i_{2,ph} - \frac{1}{\frac{n_1 r_2}{n_2} \left(\frac{1}{r_1} + \frac{n_2^2}{n_1^2 r_2} + \frac{n_3^2}{n_1^2 r_3} \right)} i_m^{(1)} \quad (12)$$

$$i_3 = i_{3,ph} - \frac{1}{\frac{n_1 r_3}{n_3} \left(\frac{1}{r_1} + \frac{n_2^2}{n_1^2 r_2} + \frac{n_3^2}{n_1^2 r_3} \right)} i_m^{(1)} \quad (13)$$

It can be seen from the expressions (11), (12) and (13) that due to the magnetizing current effect the currents i_1 , i_2 and i_3 are phase shifted to the square voltages sources. When the first switching half cycle is completed at $\omega t = \pi$ the current i_1 is positive while the currents i_2 and i_3 are negative as it is

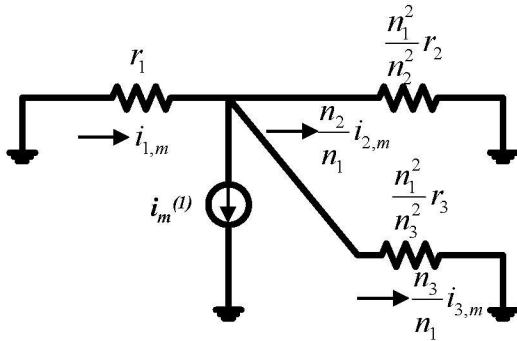


Figure 4. The equivalent circuit from Figure 3 at the fundamental harmonic of the magnetizing current, $i_m^{(1)}$.

indicated in Figure 3. If the resistances r_1 , r_2 and r_3 are equal, the magnetizing current distribution only depends on the transformer turns ratio and the secondary side circuit with higher number of turns will have higher negative current at the end of the first half cycle. This can be compensated at some extent by increasing the resonant capacitor of that circuit. In this way the resonant tank impedance will be inductive and it will reduce the peak value of the tank current due to the magnetizing current and its phase shift with respect to the input square voltage leading to decreased tank current value at the end of the first half cycle.

III. EXPERIMENTAL VERIFICATION

The performance of the proposed three port dc/dc transformer are analyzed on a prototype with 390V input voltage, V_{IN} , and 48V/5A, V_2 , and 12V/5A, V_3 , outputs. The selected switching frequency is $f_{sw} = 700$ kHz. The switches used on the primary side are IPD50R520CP (550V, 0.52Ω, 13nC) and on the secondary side IRFH5406PbF (60V, 14.4mΩ, 21nC) and IRF6631 (30V, 6mΩ, 12nC). The input and output filter capacitor values are $C_{IN} = 1.5\mu F$, $C_2 = 12\mu F$ and $C_3 = 12\mu F$. The adjusted and measured resonant capacitor values are $C_{res1, high side} = 560nF$, $C_{res1, low side} = 550nF$, $C_{res2} = 1.8\mu F$ and $C_{res3} = 2.6\mu F$. Since the total parasitic inductances L_{lk1} , L_{lk2} and L_{lk3} on current paths were not known with certainty the following procedure was used to determine the resonant capacitor values. The resonant capacitors C_{res1} were selected according to their theoretical predictions. The currents i_2 and i_3 were measured at full load and the resonant capacitors C_{res2} and C_{res3} were adjusted until the ZCS conditions at both outputs were achieved. It was then possible to calculate the total parasitic inductances on the current paths in the primary and the secondary side circuits using the equation (1): $L_{lk1} = 33nH$, $L_{lk2} = 20nH$ and $L_{lk3} = 14nH$.

One planar EE core (E18/4/10R-3F3) was used to build the transformer with two parallel windings and a turns ratio of $n_1:n_2:n_3 = 16:4:1$ achieving a transformer power density of 3.2kW/in³. A gap (560μm) is adjusted to obtain the magnetizing inductance of $L_m = 24\mu H$ needed to obtain ZVS transitions in all the switches. The total self-capacitance of the planar windings seen on the primary side is measured to be $C_p = 240pF$ which is much higher than the $C_{oss,Tr} = 63pF$ of the equivalent output capacitance of one primary side switch. Figure 5 shows the cross section of the realized transformer.

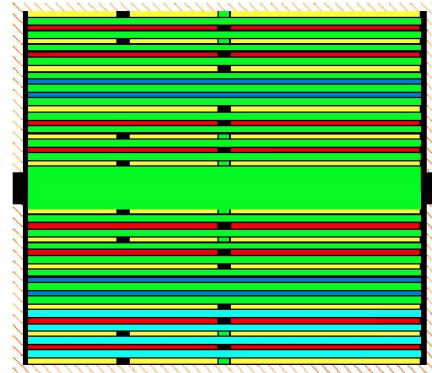
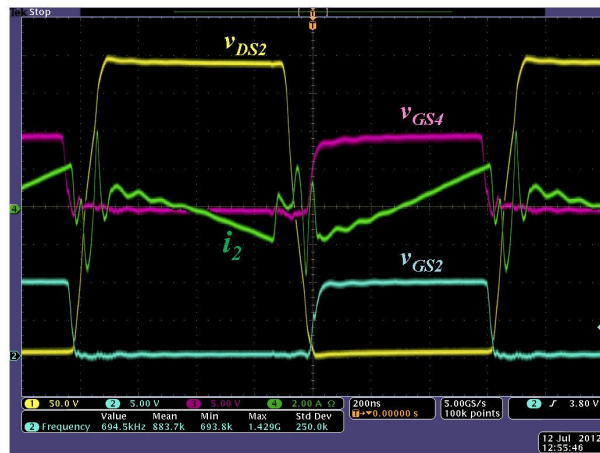
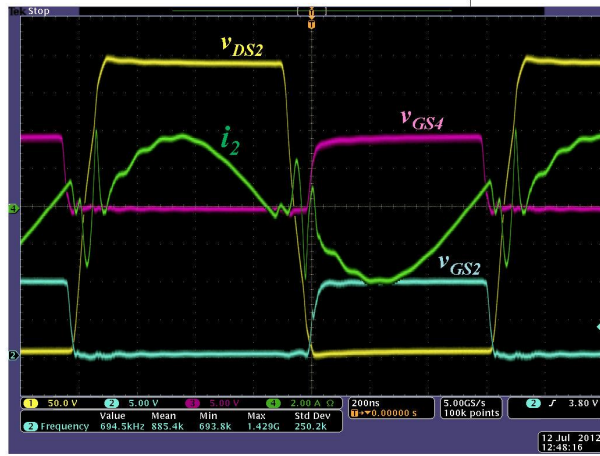
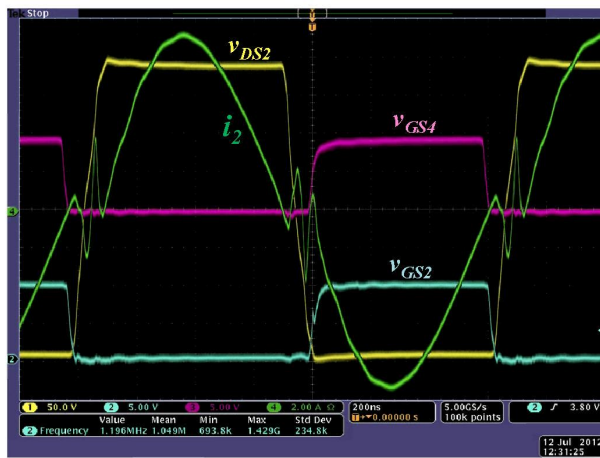
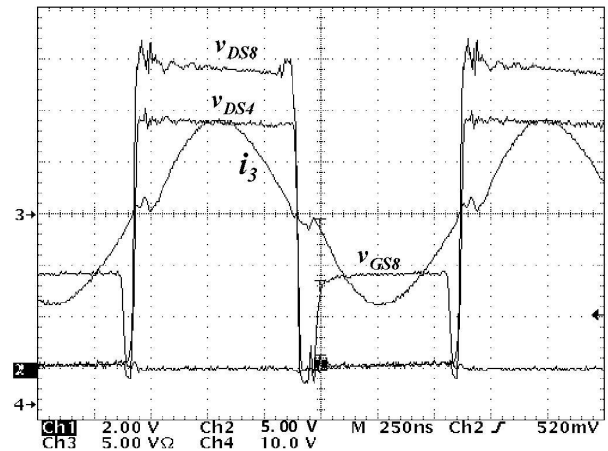


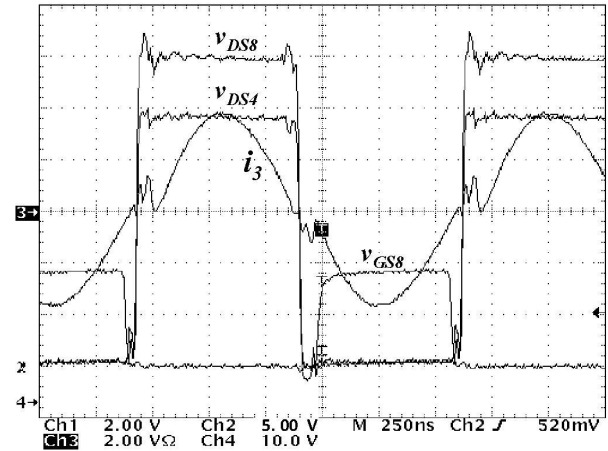
Figure 5. Cross section of the EE18/4/10R-3F3 planar transformer with two parallel 12 layer 70 μm copper PCBs.



(a)



(b)



(c)

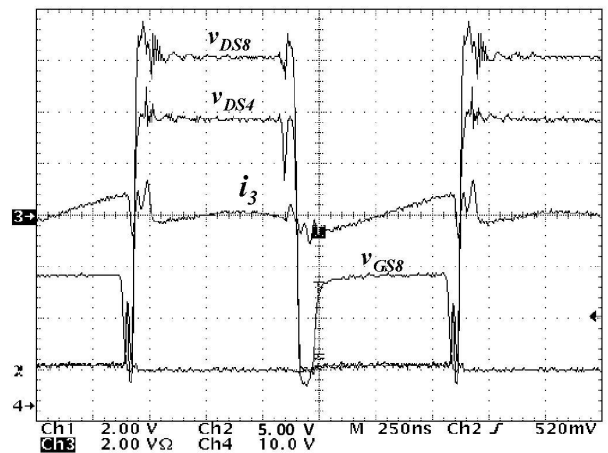


Figure 6. Experimental waveforms of the three port dc/dc transformer for the same loading conditions at both outputs: (a) full load, (b) 40% of the load and (c) no load condition. The voltage scale for the waveform v_{DS2} is 50V/div and for v_{GS2} and v_{GS4} is 5V/div. The current scale for i_2 is 2A/div.

It is worth mentioning here that the dc/dc transformer can operate in a wide range of switching frequencies. The switching frequency is selected as a tradeoff between the transformer power losses, which give maximum temperature rise in the component, and dynamic behavior of the converter. For the selected core and turns ratio a reduction in switching frequency - while in the range of frequencies valid for the

selected core material - will reduce the core and winding losses, as well as the gap value needed to obtain the desirable magnetizing inductance for ZVS. The achieved reduction of the transformer power losses can be cancelled by increasing the output power, in order to push the transformer temperature to the limit of the safe operating area and thus fully exploit the transformer.

The experimental waveforms for the steady state operation of the three port dc/dc transformer are shown in Figure 6 for both outputs are operating at full load, 40% of the load and no load conditions. In all three cases all the switches operate under ZVS condition which is not dependent on the load. At full load condition the switches in both full bridge rectifiers turn off with ZCS. A high frequency current ringing between parasitic capacitors and the leakage inductances can also be observed in the dead time interval in all i_2 current waveforms. It can also be noticed comparing Figure 6(a) and Figure 6(b) that i_2 current waveform changes as the load changes. This is due to the effect of the magnetizing current. Namely, when the magnetizing current is very small the resonant tank currents are sinusoidal, as well as the voltage drops across the resonant tanks, and remain sinusoidal for each load combination at the output. When the magnetizing current is not negligible a non-sinusoidal voltage drop across the primary side resonant tank will occur and that will alter the current distribution in the resonant tanks as it can be seen in Figure 6(b). The effect of the magnetizing current is more pronounced at light load since the output currents are lower. At no load condition, Figure 6(c), the magnetizing current is distributed among the tank currents i_1 , i_2 and i_3 . By placing higher capacitors C_{res2} and C_{res3} than the ones calculated in (2) the currents i_2 and i_3 can approach sinusoidal shape at full load. When the load decreases, the ZCS condition in switches M3, M4, M5, and M6 can be recovered at some extent by increasing their on resistances.

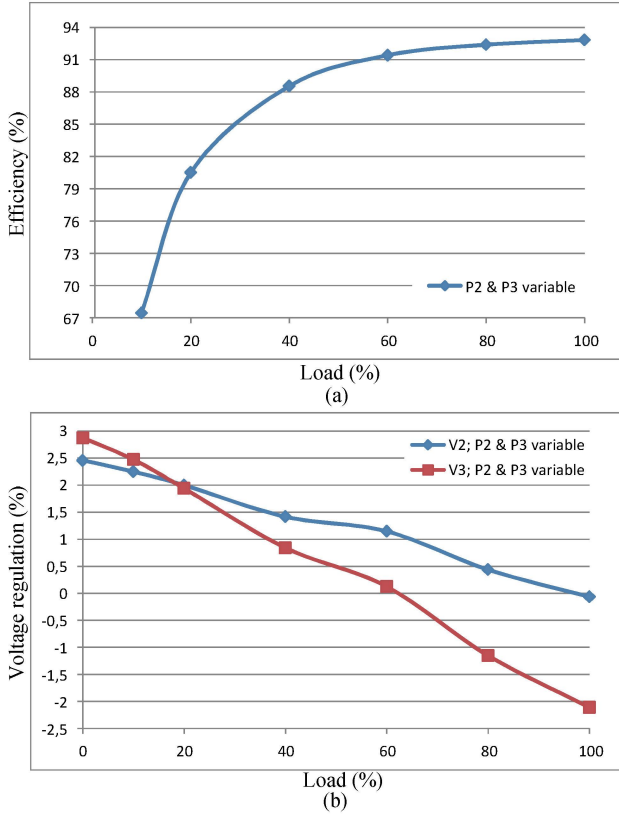


Figure 7. (a) Efficiency measurement of the three port dc/dc transformer when both output are loaded from 10% to 100% of their respective nominal loads and (b) the steady state output voltage regulation for constant input voltage.

The results of the efficiency measurements are shown in Figure 7(a) in the cases when $V_{IN}=389V$ and both outputs are changing equally from 10% of the load to full load. The maximum efficiency of 93% is measured at full load. The steady state voltage regulation performances are shown in Figure 7(b) under the same operating condition as in the case of the efficiency measurement. A very good load regulation characteristic of the converter is observed due to its inherent low output impedances. For light load to full load variation in each output the voltage V_2 variations are kept below 2.5% and in the range of -2.1% to 2.9% for the voltage V_3 .

A. Bidirectional operation

The bidirectional performances of the converter have also been tested from full load to open circuit. In case when the voltage V_2 acts as a power source the results are shown in Figure 8. All the measurements were conducted at $V_2=50.1V$. The measured efficiency figures are similar to those ones measured when the voltage V_1 acted as a power source with approximately 1.5% lower values. Once again, very good load regulation characteristics are observed. The voltage V_{IN} is maintained within the range of -0.7% to 1.2% when its load varies 100% and the V_3 voltage load is maximal and in the range of -0.7% to 0% when its load is maximal and V_3 voltage load varies 100%. Under the same operating conditions, the V_3 voltage is within the range of -1.1% to 0.5% in the first case and is maintained in the range of -0.9% to 3.4% in the second.

IV. TOLERANCE ANALYSIS

In order to check the performance of the proposed converter under parameter variations that affects the resonant frequency and may alter the ZVS-ZCS operation, a tolerance analysis of the resonant capacitor has been done. In this analysis, the duty cycle or switching frequency have been changed in order to reestablish ZCS condition.

The converter can operate properly even if the resonant capacitors are not precisely tuned to the switching frequency. In this case the switching frequency should be selected as the lower resonant frequency of the two output resonant tanks. If the duty cycle is maintained at approximately 50% as it was before the changes in resonant capacitances, a ZCS condition at the output with higher resonant frequency will be lost. The ZCS condition can be reestablished by changing the duty cycle of the driving signals at the output with higher resonant frequency in the manner that when the resonant tank current half cycle oscillation is finished the switches are turned off. In this way the rms resonant tank current value is also decreased leading to lower conduction losses. Therefore, all the rectifier switches are turned off when their corresponding currents cross zero. The primary side inverter switches are turned off together with the switches at the output with lower resonant frequency. Turn on instants of the switches M1,M3,M6,M7,M10 and M2,M4,M5,M8,M9 can be determined by sensing high and low levels of the drain-source voltage of the switch M2, respectively.

The open loop experimental waveforms that illustrate this are shown in Figure 9 in case when the resonant capacitor C_{res2} is changed to 70% of its nominal value, ($C_{res2,nom}$

=1.8 μ F). When the output V_2 is changed from no load to full load and the output V_3 is fully loaded the efficiency drop of at most 1.4% comparing to the nominal case is measured without any other changes in the circuit. On the other hand, when the duty cycle is changed as in Figure 9(b) the efficiency gain of at most +0.9% is observed comparing to the efficiency measurements when only C_{res2} is changed. However, the voltage V_2 regulation is worsening by approximately 1% in its entire load range. The voltage V_3 regulation characteristic is almost not affected by the change in the duty cycle.

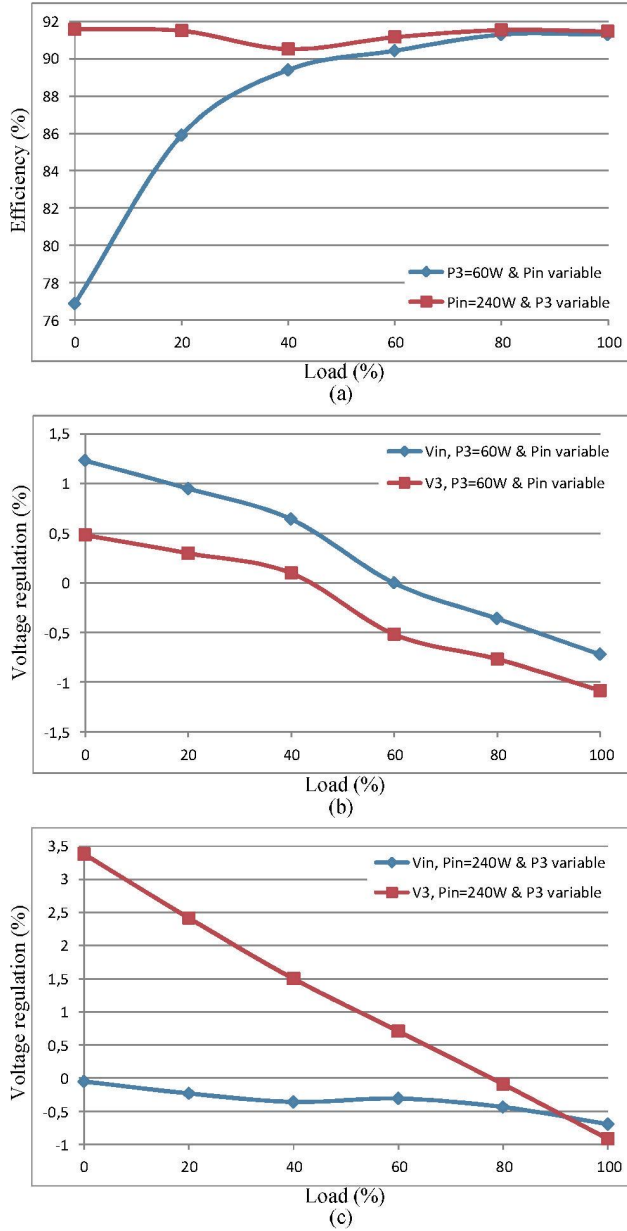


Figure 8. Bidirectional operation of the three port dc/dc transformer when V_2 acts as an input source, one output is fully loaded and the other is swept from no load to full load: (a) efficiency and (b), (c) voltage regulation characteristics.

When the resonant capacitor C_{res2} is changed to 138% of its nominal value the switching frequency has to be changed to 600 kHz as well as the duty cycle of the driving signals of the switches M7, M8, M9 and M10, Figure 10. When the output V_2 is changed from no load to full load and the output V_3 is fully loaded the efficiency loss of at most -1.1% is observed comparing to the nominal case without any other changes in the circuit. When the duty cycle and frequency are changed, the efficiency loss of at most -0.5% is observed comparing to the efficiency measurements when only C_{res2} is changed. For light load to full load variation at V_2 output, its regulation characteristics is slightly deteriorated after the frequency and duty cycle are changed while the voltage V_3 regulation characteristics is almost not affected. A photo of the prototype is shown in Figure 11.

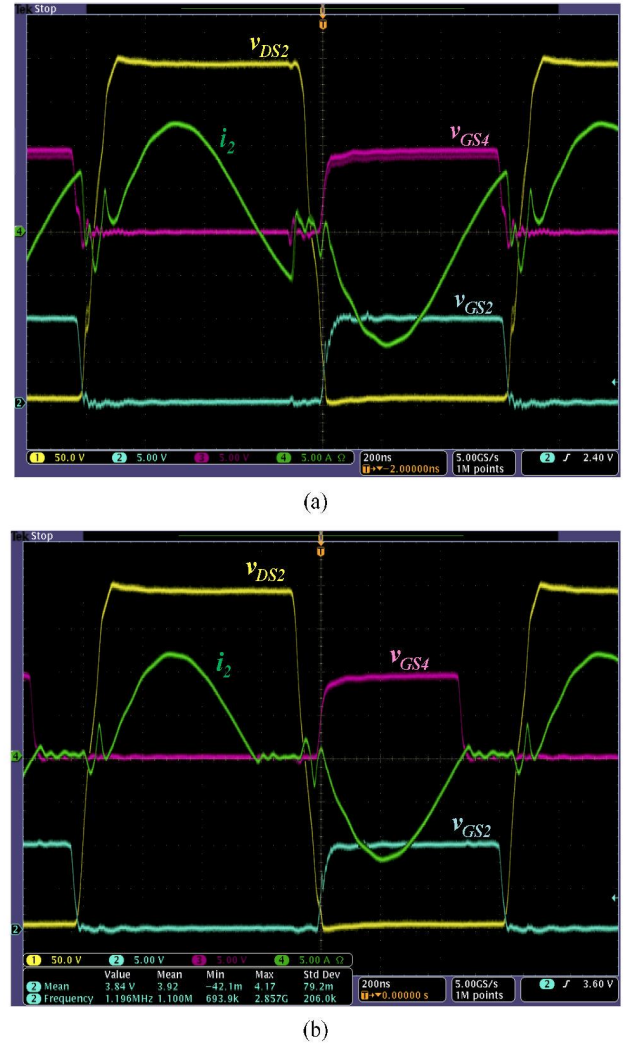
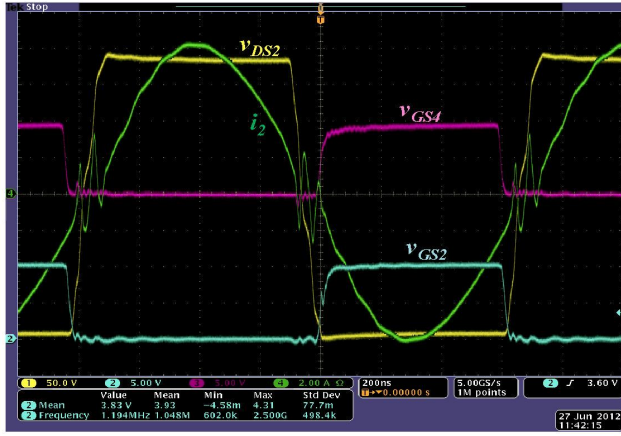
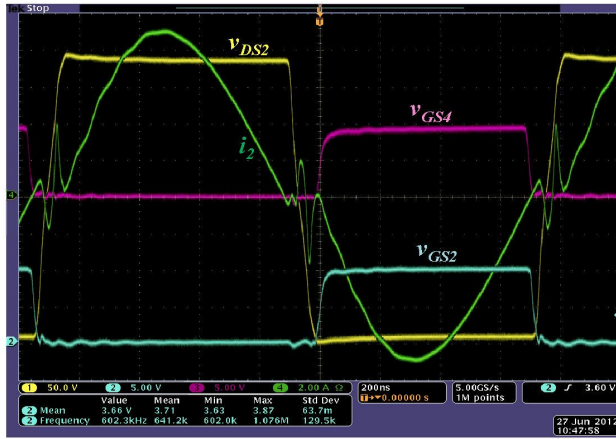


Figure 9. Experimental waveforms when C_{res2} is decreased 70% of its nominal value: (a) without any change in the switching frequency or driving signals and (b) with adjusted the duty cycle of the driving signals of the switches M3, M4, M5, M6. The voltage scale for v_{DS2} is 50V/div and for v_{GS2} and v_{GS4} is 5V/div. The current scale for i_2 is 5A/div.



(a)



(b)

Figure 10. Experimental waveforms when C_{res2} is increased 138% of its nominal value: (a) without any change in the switching frequency or driving signals and (b) with adjusted the switching frequency (to 600kHz) and the duty cycle of the driving signals of the switches M7, M8, M9, M10. The voltage scale for v_{DS2} is 50V/div and for v_{GS2} and v_{GS1} is 5V/div. The current scale for i_2 is 2A/div.

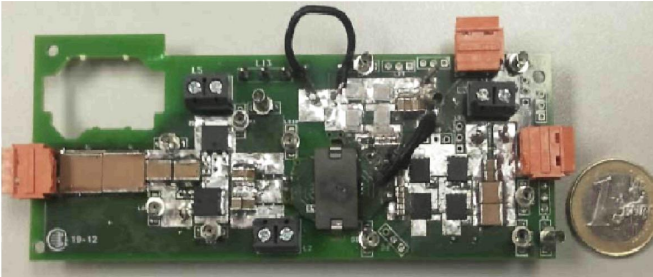


Figure 11. Photo of the three port bidirectional 300W 700 kHz prototype.

V. CONCLUSIONS

In this paper, a novel multiple port dc/dc bidirectional transformer concept is proposed. The concept is based on the SRC topology operating just at the resonance frequency. In this way, the input voltage regulation capability is lost but high power density operation at constant switching frequency is possible. The converter features the virtual elimination of the power transistor switching losses in all the inverter

bridges; ZVS and nearly ZCS are achieved in all the switches. This allows for higher switching frequencies to be adopted and, consequently, reduce the size of the high frequency transformer, which is the only magnetic component in the converter. Full bridge and half bridge inverter/rectifier cell combinations are possible depending on the specifications. A very good load regulation characteristic of the converter is observed due to its inherent low output impedances. The converter performances are experimentally verified on a 300W, 700 kHz prototype with 390V input voltage and 48V and 12V output voltages. The transformer is built on one EE18 core and its power density is 3.2kW/in³. The maximum efficiency of 93% is measured at full load. The bidirectional operation is validated from no load to full load with similar performance. The tolerance analysis has shown that the variation of the resonant capacitor C_{res2} in the range of 70% to 138% of its nominal value causes small efficiency drop and very small deterioration of the voltage regulation characteristics, despite the fact that the switching frequency is not adapted to the resonance frequency variation. If it is necessary, the resonant capacitors' tolerances could be compensated by precise selection of the switching frequency and duty cycle in a closed loop operation.